

Role of Deformation-induced Lipid Trafficking in the Prevention of Plasma Membrane Stress Failure

Nicholas E. Vlahakis, Mark A. Schroeder, Richard E. Pagano, and Rolf D. Hubmayr

Pulmonary and Critical Care Medicine Division, Mayo Clinic and Foundation, Rochester, Minnesota

Cells experience plasma membrane stress failure when the matrix to which they adhere undergoes large deformations. In the lung, such a mechanism might explain mechanical ventilation–associated cell injury. We have previously shown that in alveolar epithelial cells, deformation induces lipid trafficking to the plasma membrane, thereby accommodating the required increase in the cell surface area. We now show that cell wounding is strain amplitude and rate dependent and that under conditions of impaired exocytosis strain-induced cell wounding is significantly increased. In addition, the susceptibility of cells to mechanical injury was not correlated with changes in cell stiffness. Using a dual-labeling technique, we differentiated between cell populations that were reversibly and irreversibly injured and showed that interventions that impair deformation-induced lipid trafficking also reduce the likelihood of plasma membrane resealing. Our findings suggest that cell plasticity and remodeling responses such as deformation-induced lipid trafficking are more important for cytoprotection from strain injury than are the innate mechanical properties of the cell. We also conclude that in deformation experiments, tests of cell membrane integrity cannot be interpreted as tests of cell viability because an intact plasma membrane after deformation does not mean that no injury had occurred.

Keywords: exocytosis; plasma membrane wounding; plasma membrane resealing; ventilator-induced lung injury

Cells experience plasma membrane stress failure when the matrix to which they adhere undergoes large deformations (1–3). In the lung, this mechanism might explain epithelial and endothelial cell disruptions associated with high tidal volume mechanical ventilation (4, 5). To simulate alveolar volume change during mechanical ventilation, alveolar epithelial cells are grown on malleable substrata, which when stretched deform the overlying cells, resulting in a large surface-to-volume ratio (3, 6, 7). In fibroblasts and neurons, unfolding of excess plasma membrane and exocytosis allow cells to increase their surface area while protecting the lipid bilayer from lytic tension (8, 9). Recently, we reported that in alveolar epithelial cells, intracellular lipids are trafficked to the plasma membrane after substratum stretch (7). This deformation-induced lipid trafficking (DILT) is vesicular in nature and energy and strain amplitude dependent and accommodates deformation-induced changes in cell surface area.

These prior studies led us to postulate that DILT is important for protection against deformation-related cell injury.

(Received in original form March 14, 2002; accepted in final form July 22, 2002)

Funded by a Glaxo-Wellcome Research Fellowship grant, a grant from the Brewer Foundation, and National Institutes of Health grants GM 22942 and HL-63178.

Correspondence and requests for reprints should be addressed to Nicholas E. Vlahakis, M.D., Stable 8-62, Mayo Clinic, 200 First Street SW, Rochester, MN 55905. E-mail: vlahakis.nicholas@mayo.edu

This article has an online data supplement, which is accessible from this issue's table of contents online at www.atsjournals.org

Am J Respir Crit Care Med Vol 166, pp 1282–1289, 2002

Originally Published in Press as DOI: 10.1164/rccm.200203-207OC on July 25, 2002

Internet address: www.atsjournals.org

To test this hypothesis, we measured the susceptibility of alveolar epithelial cells to stretch amplitude and rate-induced plasma membrane wounding. Cell wounding is commonly assessed using fluorescently labeled, membrane-impermeable macromolecules such as fluorescein-labeled dextran (FDx) (2, 3, 10–12). FDx enters the cell through plasma membrane breaks and is retained in the cytoplasm when the membrane defect reseals (11, 13, 14). However, if a wounded cell fails to reseal a plasma membrane defect, FDx cannot be retained and the cell cannot be distinguished from an uninjured cell. We present here a novel dual-labeling technique using first FDx and, after stretching, propidium iodide (PI), which labels the nuclei of injured and nonresealed cells. Using this approach, we were able to identify three cell populations: (1) wounded and resealed cells, (2) wounded cells that had not resealed, and (3) uninjured cells with intact plasma membranes. Our findings highlight that live–dead exclusion assays performed at the end of a deformation experiment might be both false positive (lethal wounding is not distinguished from wounding and resealing) and false negative (wounded and nonresealed cells might not retain exclusion dyes).

Additional experiments were performed under conditions of impaired exocytosis, induced by cold temperature or cholesterol depletion. These interventions, which impaired DILT, also made cells more prone to injury and altered the cells' resistance to shape change. Because changes in cell mechanical properties might determine a cell's susceptibility to injury, we measured the effects of cytoskeleton active agents on DILT along with their effects on apparent cell stiffness. Based on these measurements, we conclude that remodeling responses such as DILT are more important for protecting the plasma membrane against stress failure than are the inherent strength and organization of stress-bearing elements such as the subcortical cytoskeleton.

METHODS

Experimental Design for Determination of Plasma Membrane Breaks

When deformation-induced breaks occur, fluorescently labeled molecules—typically membrane impermeable—enter the cell along a concentration gradient. Cells were incubated with FDx (70 kD; Fluka, Milwaukee, WI) and then strained as described later here. After cell deformation, cells were incubated with PI (668 D; Sigma, St. Louis, MO) or in a few experiments with unesterified calcein (622 D; Molecular Probes, Eugene, OR). Cells with FDx or nuclear PI labeling were counted in five low-power ($\times 40$) microscope fields in each culture well and were tabulated as a percentage of the total cells counted. FDx-positive/PI-negative cells were considered wounded and resealed, and PI-positive/FDx-negative cells were considered wounded and nonresealed.

Alveolar Epithelial Cell Culture

Human A549 (passages 78–88), rat L2 (passages 27–40) (American Type Culture Collection, Rockville, MD), and Day 5 primary rat alveolar epithelial cells (AEC) were grown on six-well culture plates (Bioflex; Flexcell International Corporation, McKeesport, PA) with a flexible

silicoelastic membrane base (*see* online data supplement [METHODS section]).

Cell Strain Devices

Two strain devices were used, both of which have been previously described (1, 7) (*see* online data supplement [METHODS section]). For cell injury experiments, strain amplitudes of 3–25% and rates of 1–140% per second were studied. For lipid trafficking experiments, a single stretch of $25 \pm 2.8\%$ was applied to the cells.

Labeling of Lipid Membranes

The methods have been previously described (7). Briefly, intracellular membranes of A549 and/or Day 5 AEC cells were fluorescently labeled by incubating with $2 \mu\text{M}$ of FM1-43. The fluorescence intensity of the cell decreases after exocytosis to the plasma membrane. In separate experiments, exocytosis was measured before and after deformation under the following conditions: (1) cold temperature (4°C), (2) plasma membrane cholesterol depletion (β -methyl-cyclodextrin; Sigma), and (3) cytoskeletal active agents (cytochalasin D, paclitaxel, and colchicine; Sigma).

Cell Imaging

For cell injury experiments, cells were viewed immediately after injurious deformation using a $40\times$ water immersion objective lens to visualize FDx or calcein and PI. For lipid trafficking experiments, cells were imaged using an argon ion laser scanning confocal microscope (Fluoview3; Olympus, Melville, NY). One-micron optical sections were obtained using a $40\times$ water immersion objective lens (Olympus). Fluorescent labels were excited with blue laser light and emission wavelengths collected simultaneously by green and red filters (Olympus). Membrane fluorescent intensity measurements were calculated with an image display and manipulation package (15) from a single image slice through the middle of the cell acquired in both its undeformed and deformed states.

Magnetic Twisting Cytometry

The methods have been previously described (16, 17). Ferromagnetic (Fe_3O_4) microbeads ($4.5 \mu\text{m}$ in diameter) were coated with a synthetic arginine-glycine-aspartate synthetic peptide (RGD) peptide (Telios Pharmaceuticals, Inc., San Diego, CA), added to each well, and placed into the magnetic twisting cytometer. The beads were magnetized in the horizontal direction. A magnetic “twisting” field, the strength of which defines local stress, was applied in the vertical direction to twist the beads upward, and apparent cell stiffness was calculated (17).

Statistical Analysis

Fluorescent intensity measurements and cell injury percentages are presented as means and SD. Statistical comparisons between experimental conditions were made using the Student *t* tests for paired observations. Analysis of variance was used to determine strain effect on the percentage of wounded cells across a different strain amplitude, strain rate, and temperature. Statistical significance was assumed at $p < 0.05$ with respect to a two-tailed probability distribution.

RESULTS

Substratum Strain Induces Plasma Membrane Wounds in Adherent Alveolar Epithelial Cells

The fractions of injured cells and their resealing responses in different alveolar epithelial culture systems after exposure to a single large deforming stress are shown in Figure 1. A549 ($n = 5$, 27 wells), L2 ($n = 2$, eight wells), and rat alveolar epithelial cells ($n = 2$, 12 wells) were rapidly stretched by 25%. The susceptibility to stretch-induced wounding and the probability of subsequent resealing varied across cell types. The fraction of wounded A549, L2, and primary rat alveolar epithelial cells was 6%, 21%, and 46%, respectively. The rates of resealing were 38%, 78%, and 21%, respectively.

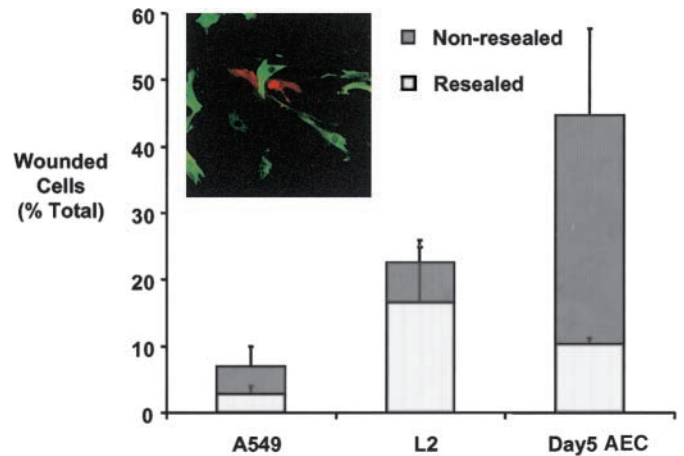


Figure 1. Cell wounding in alveolar epithelial cells after a single substratum deformation of 25% amplitude with a strain rate of 140% per second. Each bar on the graph represents total cell wounding divided into those cells that were able to reseat (FDx positive/PI negative) and those unable to reseat (PI positive/FDx negative). The *inset* fluorescent micrograph illustrates a confluent monolayer of alveolar epithelial cells with the injured and resealed cells being *green* and the injured and nonresealed cells being *red*. Uninjured cells lay in between these cells and are not labeled with fluorescent dyes.

Plasma Membrane Resealing after Cell Wounding Maintains Cell Viability

Cell viability was determined for both FDx- and PI-positive A549 cells and Day 5 primary rat alveolar epithelial cells ($n = 3$, eight wells). After deformation, the adherent cells were reincubated with fresh nutrient media. Twelve and 24 hours later, the number of FDx- and PI-positive cells was recounted. There was no difference ($p > 0.05$) in the number of FDx-positive cells when compared immediately after stretch and 12 and 24 hours after stretch; however, no PI-positive cells were seen. Because PI is itself cytotoxic, we repeated these experiments using a nontoxic second label, namely unesterified calcein. No calcein-positive cells could be identified after 12 or 24 hours, suggesting that failure to reseat plasma membrane wounds rapidly is a lethal event.

Plasma Membrane Wounding Is Strain Amplitude and Strain Rate Dependent

Figure 2A shows that the number of A549 cells that sustained plasma membrane breaks after a single rapid stretch increases as a function of strain amplitude. When compared with no strain, cells strained at amplitudes of 9% ($n = 3$, 18 wells), 18% ($n = 18$, 63 wells), and 25% ($n = 21$, 101 wells) had a 1-fold, 3.4-fold, and 5.2-fold increase ($p < 0.01$) in cell wounding, respectively. At amplitudes of 9% or less, there was no difference in wounding compared with unstrained cell populations. Figure 2B shows that this dependence of wounding on strain amplitude was also demonstrable in L2 cells ($n = 2$, six wells for each strain amplitude) and in primary Day 5 AEC cells (data not shown). L2 cells and primary alveolar epithelial cells were more susceptible to wounding than A549 cells.

Figure 3 ($n = 4$, 12 wells) shows that in A549 and L2 cells, the susceptibility to injury varies not only with strain amplitude but also with strain rate. In A549 cells (Figure 3A), at the highest strain rate of 140% per second, a single stretch of 25% produced two times (4.9% versus 2.6%, $p < 0.0001$) and three times (4.9% versus 1.3%, $p < 0.0001$) more wounding than at rates of 40%

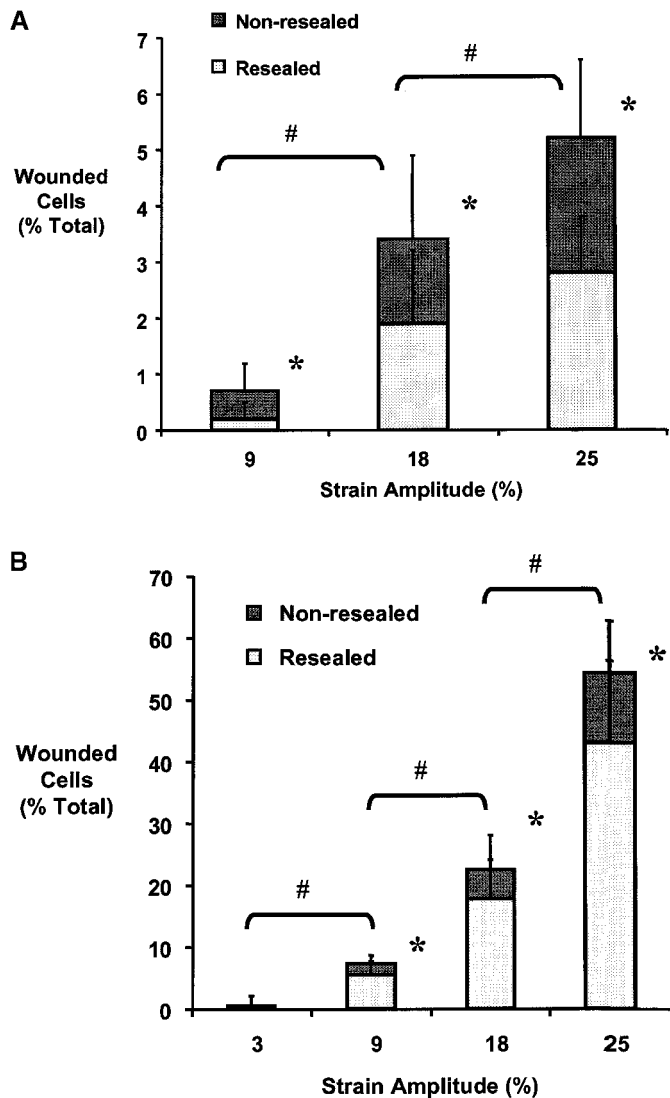


Figure 2. Deformation-induced cell wounding increases with increasing strain amplitude. Strain rate was set to 140% per second. (A) A549 cells. (B) L2 cells. * $p < 0.05$ compared with no strain; # $p < 0.05$ comparison between indicated strain amplitudes.

per second and 12% per second, respectively. When stretched at a rate of 3% per second, a 25% stretch produced no irreversible cell injury. Similarly, in L2 cells (Figure 3B), a single stretch of 25% with a strain rate of 140% per second resulted in 0.7 times (23.1% versus 15.9%, $p < 0.0001$) and 5.5 times (23.1% versus 4.2%, $p < 0.0001$) more wounding than at rates of 40% per second and 12% per second, respectively.

Cold Temperature and Cholesterol Depletion Inhibits DILT

To test whether vesicular lipid trafficking is important for protecting cells from mechanical injury, we first had to demonstrate that exposure to cold temperature and cholesterol depletion indeed inhibited DILT. The effects of cooling on the stretch-related decrease in FM1-43 fluorescence (a marker of exocytosis) in A549 cells (two experiments, six cells) and in primary rat alveolar epithelial cells (two experiments, six cells) are shown in Figure 4A. At room temperature, a single stretch of 25% caused an eightfold and a threefold decrease in FM1-43 fluorescence, compatible with a significant exocytic response. Also note that at 4°C, the same stretch produced no significant change

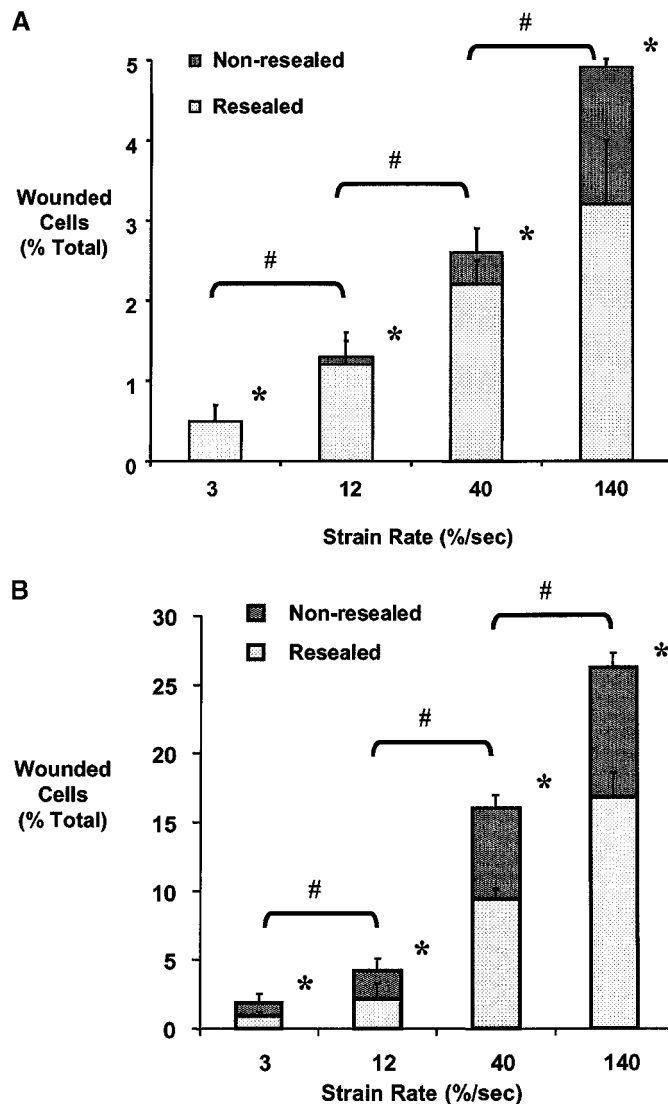


Figure 3. Deformation-induced cell wounding increases with increasing strain rate. Strain amplitude was set to 25%. (A) A549 cells. (B) L2 cells. * $p < 0.05$ compared with no strain; # $p < 0.05$ comparison between indicated strain rates.

in FM1-43 fluorescence, consistent with inhibition of DILT. Figure 4B shows that treatment of A549 cells ($n = 3, 18$ cells) and alveolar epithelial cells ($n = 3, 11$ cells) with β -methyl cyclodextrin also results in inhibition of DILT compared with untreated and stretched epithelial cells. β -Methyl-cyclodextrin was found to reduce the total cholesterol content of A549 cells by up to 45% (data not shown).

Cholesterol Depletion Increases the Susceptibility of Alveolar Epithelial Cells to Stretch-related Injury

Having demonstrated inhibition of DILT, we next sought to measure the effect of this inhibition on the cells' susceptibility to deformation-related wounding. The incidence of stretch-related plasma membrane wounding was significantly increased in cholesterol-depleted cells compared with placebo-treated controls. In A549 cells and primary alveolar epithelial cells, cholesterol depletion raised the fraction of wounded cells from $1.4 \pm 1.5\%$ to $4.0 \pm 1.3\%$ ($p < 0.0001$; Figure 5A) and from $49 \pm 3.2\%$ to $59 \pm 2\%$ ($p < 0.0003$; Figure 5B), respectively. Furthermore,

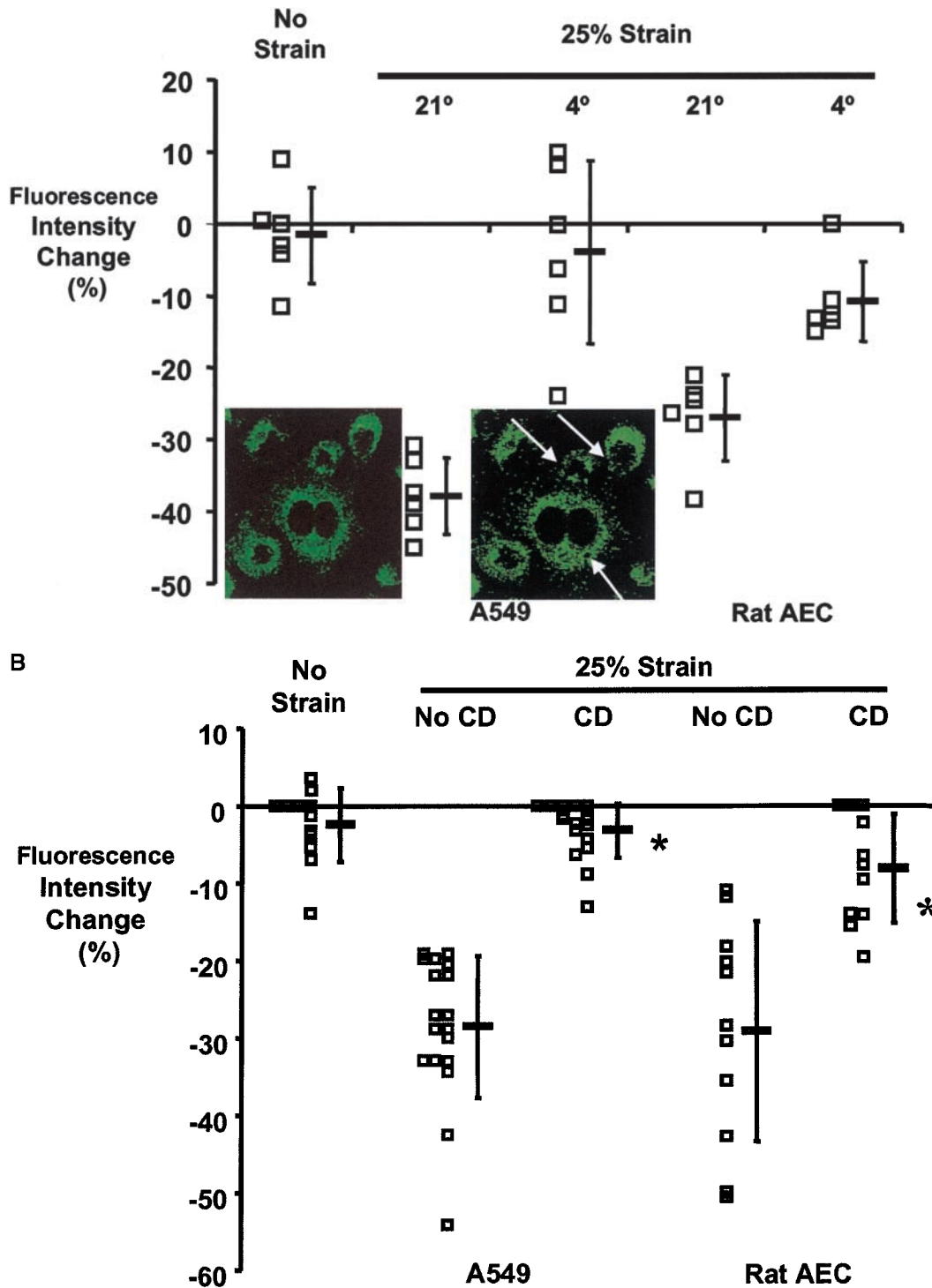


Figure 4. Low temperature and cholesterol depletion inhibit lipid trafficking to the plasma membrane in both A549 and primary rat alveolar epithelial cells after a single held 25% substratum deformation. (A) At 21°C, the intensity of FM1-43 labeling within the cell decreases consistent with lipid exocytosis. The inset confocal micrograph illustrates the loss of FM1-43 (arrows) after stretch. At 4°C, this response is inhibited ($p < 0.001$). (B) β -Methyl cyclodextrin inhibits (in both A549 and alveolar epithelial cells) DILT to the plasma membrane. Each data point represents a single cell and its change in fluorescence between the unstretched and stretched state. The nonstretched cells served as a time control for lipid trafficking and photobleaching effects of fluorescent and laser light. CD, β -methyl cyclodextrin.

the fraction of wounded cells that healed was substantially reduced after cholesterol depletion. The resealing rate of wounded and cholesterol depleted A549 cells was $46 \pm 7.7\%$ compared with $73 \pm 30.3\%$ in normal controls ($p < 0.006$; Figure 5A). Similar effects were observed in alveolar epithelial cells in which cholesterol depletion lowered the resealing rate from $24 \pm 3.4\%$ to $15 \pm 2\%$ ($p < 0.0004$; Figure 5B).

Cooling Increases the Susceptibility of A549 Cells to Stretch-related Injury

We have previously demonstrated that cooling changes the mechanical properties of cells and increases their susceptibility to

deformation-related injury (1); however, in prior experiments, we had assessed injury solely on the basis of FDx retention and thereby implicitly assumed a lack of temperature effect on the resealing rate. Figure 6 shows that this assumption is incorrect. Compared with 37°C, low temperature increased the number of cells with stretch-induced wounding. At the 3% per second, 12% per second, 40% per second, and 140% per second strain rate, low temperature increased total wounding by 2.5-fold, 4-fold, 4-fold, and 3.5-fold, respectively ($p < 0.001$). In addition, low temperature also decreased the number of cells that resealed stretch-induced plasma membrane breaks. At the 3% per second, 12% per second, 40% per second, and 140% per second

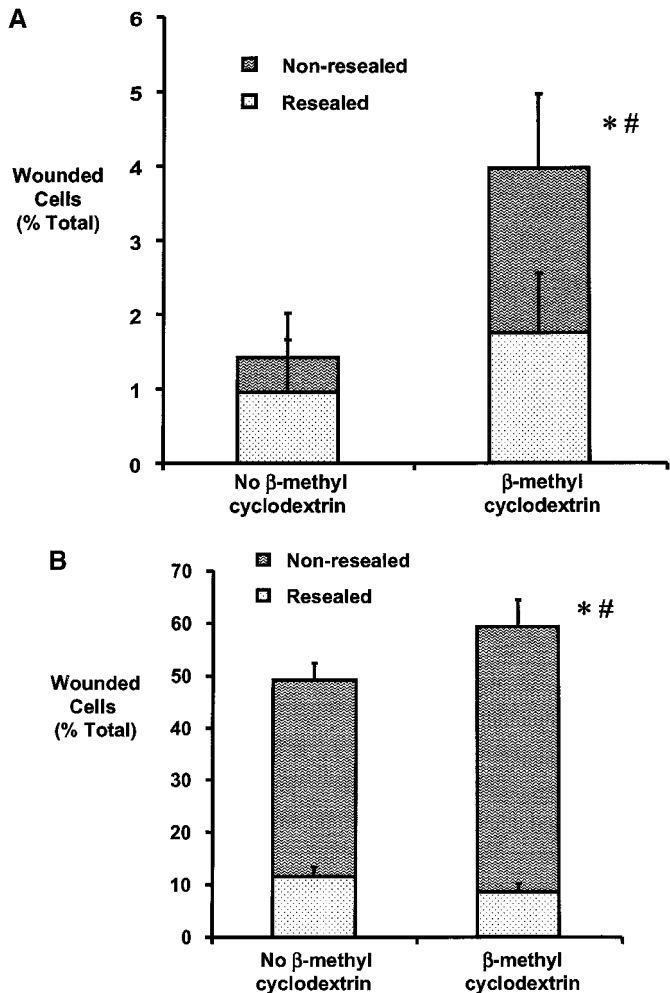


Figure 5. Cholesterol depletion results in increased stretch-induced wounded cells (* $p < 0.05$) and cells that do not reseal (* $p < 0.05$) in both (A) A549 and (B) Day 5 primary rat alveolar epithelial cells. Cells were deformed with a single 25% amplitude, 140% per second strain rate deformation held for 90 second.

strain rate, low temperature increased the proportion of nonresealed plasma membrane breaks by 40-fold, 9.5-fold, 5-fold, and 2-fold, respectively ($p < 0.001$). Therefore, analyses that are entirely based on FDx retention can substantially underestimate the effects of an intervention such as cooling on stretch injury.

Inhibition of DILT Increases the Susceptibility to Stretch Injury Independent of the Cells' Resistance to Shape Change

We had previously speculated that the inherent mechanical properties of cells determine their susceptibility to deformation injury (1, 3). To test this hypothesis, we measured the effects of cholesterol depletion, cooling, and cytoskeletal active agents on apparent A549 cell stiffness as shown in Figure 7. These interventions have diverse effects on the cells' resistance to a shape change; however, these same cytoskeleton active agents all raise the cells' susceptibility to stretch injury. Figure 8 shows that after microfilament depolymerization with cytochalasin D ($n = 3$, nine wells), the percentage of wounded A549 cells increased from $3.8 \pm 0.8\%$ to $6.0 \pm 1.4\%$ ($p < 0.0001$), whereas there was an increase in the proportion of nonresealed cells by 3-fold ($p < 0.0001$). Changes in microtubular assembly (colchicine; four experiments, 12 wells) and disassembly (paclitaxel; four experi-

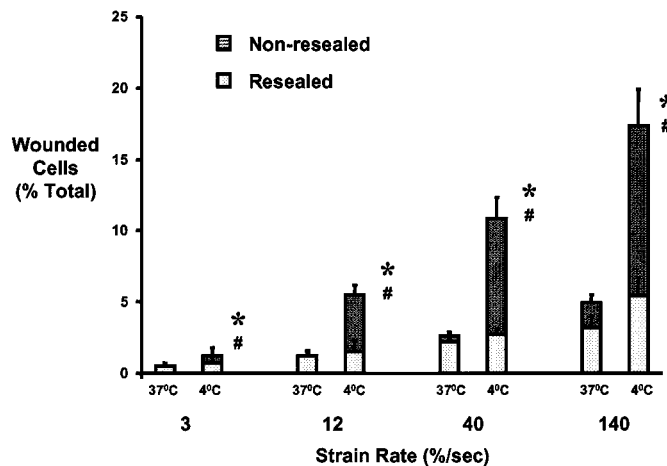


Figure 6. Low temperature results in increased numbers of stretch-induced wounded cells (* $p < 0.05$) and cells that do not reseal (* $p < 0.05$). A549 cells were stretched at 4°C and were compared with paired wells stretched at 37°C at 3% per second, 12% per second, 40% per second, and 140% per second strain rates.

ments, 15 wells) resulted in a 34% increase ($5.1 \pm 1.9\%$ to $8.6 \pm 1.7\%$, $p < 0.0001$) and a 29% increase ($4.4 \pm 0.7\%$ to $5.8 \pm 1.1\%$, $p < 0.001$), respectively, in the number of wounded cells. Both colchicine and paclitaxel inhibited resealing, increasing the proportion of cells that did not reseal by 1.5-fold ($p < 0.001$).

Strikingly, this apparent discordance in findings is explained by the fact that these agents all impair DILT (Figure 9). In the presence of cytochalasin D, colchicine, and paclitaxel, DILT was inhibited 6-fold, 12-fold, and 11-fold, respectively ($p < 0.0001$, 10 cells) as compared with cells stretched without cytoskeletal agents present.

DISCUSSION

In this study, we show that inhibition of DILT by low temperature and cholesterol depletion results in an increased probability of cell wounding. This finding highlights the importance of lipid

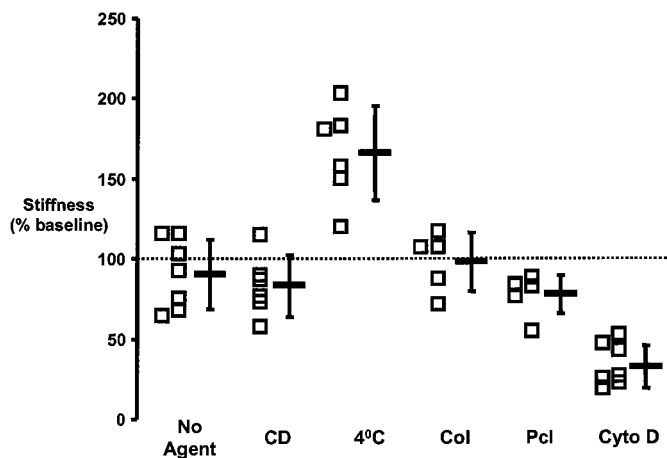


Figure 7. Change in apparent stiffness in A549 cells exposed to cyclodextrin, low temperature, and cytoskeletal agents. These agents all have differing effects on cell stiffness. CD = β -methyl cyclodextrin; Col = colchicine; Pcl = paclitaxel; Cyto D = cytochalasin D.

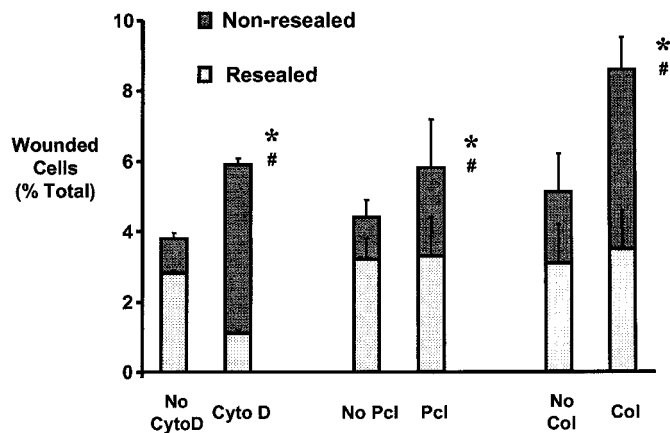


Figure 8. Treatment of A549 cells with cytoskeletal active agents results in increased numbers of stretch-induced wounded cells (* $p < 0.05$) and cells that do not reseal (* $p < 0.05$). A549 cells were stretched in the presence of cytoskeletal active agents and compared with paired wells stretched without these agents at an amplitude of 25% and a strain rate of 140% per second. Cyto D = cytochalasin D; Pcl = paclitaxel; Col = colchicines, each at 1 μ M for 1 hour before stretch and fluorescence measurement.

exocytosis as a means to accommodate deformation-induced changes in cell shape and in turn to prevent plasma membrane breaks. We also show that despite the opposite effects of low temperature and cholesterol depletion on apparent cell stiffness, the probability of wounding increased. Similarly, the probability of cell wounding increased after both increases and decreases in cytoskeletal stiffness. These findings are explained, at least in part, by their inhibition of vesicular lipid trafficking to the plasma membrane. We therefore conclude that a dynamic remodeling process such as DILT is a more important determinant of cell

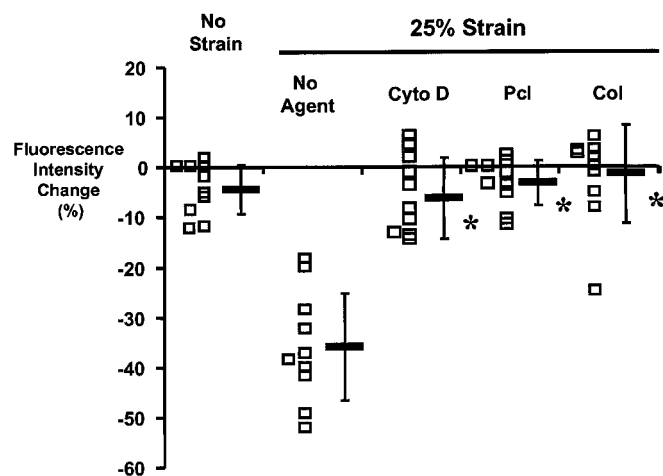


Figure 9. Perturbation of cellular microfilaments (cytochalasin D) or microtubules (colchicine and paclitaxel) inhibits lipid trafficking to the plasma membrane in A549 cells after a single, held 25% substratum deformation. Each data point under the 25% strain bar represents a single cell and its change in fluorescence between the unstretched and stretched state. The nonstretched cells served as a time control for lipid trafficking and photobleaching effects of fluorescent and laser light. Cyto D = cytochalasin D; Pcl = paclitaxel; Col = colchicines, each at 1 μ M for 1 hour before stretch and fluorescence measurement.

wounding than the mechanical properties of the cell's stress-bearing elements before deformation.

By using a dual-labeling technique for identifying plasma membrane wounding, we also show that substratum deformation results in plasma membrane breaks that either reseal (maintaining cell viability) or do not reseal (resulting in cell death). We demonstrate that inhibition of DILT not only increases the probability of cell wounding but also decreases the probability of wound resealing, suggesting that DILT plays a role not only in wound prevention but also in wound resealing.

Importance of Defining Cell Injury as Wounding or Resealing

Although the distinction between wounded and resealed and wounded and nonresealed cells seems obvious, it is rarely made in the literature when analyzing the etiologic factors and biologic consequences of cellular deformation (2, 11, 18). As a result, cells that are wounded and resealed are often considered “injured” without accounting for those cells that were wounded and not resealed. The implications of these findings are substantial.

First, this distinction facilitates a more accurate assessment of factors determining either wounding or resealing. This is illustrated by our results regarding the effect of strain amplitude and strain rate. If total cell wounding is not accounted for, one might conclude that resealing increases proportionally with both interventions; however, by measuring total wounding, it is appreciated that they have opposite effects on the probability of resealing. The biologic reason for this is unclear and warrants further study but does suggest that wounding per se might have determinants that are separate from resealing.

Second, the determinations of cell death by the use of cellular markers depending on plasma membrane integrity potentially are unsuitable for deformation experiments. Many of the cells considered to be “dead” might merely be injured with resealed plasma membrane breaks. Numerous deformation experiments to date have used such an approach and now must be reassessed in light of this new data (2, 11, 12, 18). This in turn has “downstream” implications regarding interpretation of deformation-induced cellular responses. For example, protein measurement will be “confounded” by differing contributions from the irreversibly wounded and resealed cell populations (19). Thus, the degree of wounding and resealing must be established for all experimental conditions and deformation parameters (including strain rate).

Third, although the study of alveolar epithelial biology using cell lines has limitations (20), our data support the notion that important biologic phenomena are shared by alveolar epithelial cell lines and primary cell cultures, particularly as it pertains to studies of cell injury and repair mechanisms *in vitro*. We studied human A549 cells, rat L2 cells, and rat primary alveolar epithelial cells and found that the determinants of DILT, wounding, and resealing were similar in primary cells and cell lines. It is of note that injured primary cells were less likely to reseal than wounded A549 and L2 cells. The reasons underlying this remain to be determined, but such factors as differences in state of polarization and interconnectedness, rate constant for cytoskeletal remodeling and vesicular trafficking, or more global differences in mechanosensing and mechanotransduction might all play a role.

Cell Plasticity Is More Important for Determination of Wounding Than the Mechanical Properties of the Stress-Bearing Elements

The cell possesses numerous biologic strategies to adapt to shape changes resulting from mechanical forces, many of which have been recently reviewed in detail (21, 22). The cytoskeleton is

considered the key stress-bearing element of the cell, and the integrity of the plasma membrane, an envelope-like structure serving as a barrier between the intracellular and extracellular environments, is essential for cell survival and function (9). Adherent cells have been modeled as tensegrity structures as a means to explain deformation responses and determinants of cell injury. The cell is depicted as an integrated network of compression struts and tensional guide wires (the cytoskeleton) that is connected to the extracellular matrix through integrins. When deformed, the cytoskeleton undergoes conformational rearrangements and increased tension to adapt to the resultant cell shape change (17, 23). An intact cytoskeleton is thought to fortify the plasma membrane (24), and as long as sufficient lipid surface is available, plasma membrane stress failure can be prevented.

We have previously postulated on the adaptive responses of the lipid surface to deforming stress in alveolar epithelial cells (3). First, the cell might unfold plasma membrane "ruffles," thus preventing any increase in plasma membrane tension. Second, the plasma membrane, once unfolded, might be able to accommodate a 2–3% lateral strain before yielding (8, 9, 25). Third, if these responses are overwhelmed, the plasma membrane might either undergo stress failure or further adapt its stress-bearing elements to prevent plasma membrane breaks. For example, after deformation, the protein components of actin-extracellular matrix adhesions remodel (26), forming larger and stronger focal adhesion complexes (27). Lipid trafficking to the cell surface is another such adaptive mechanism and has been demonstrated in numerous *in vitro* cell systems using various deformation profiles (8, 9, 13, 25, 28). We have shown that this phenomenon also occurs in alveolar epithelial cells (7). We now demonstrate that after inhibition of DILT by cholesterol depletion and cold temperature, the probability of wounding is increased. These interventions have opposite effects on cell stiffness: decreased by plasma membrane cholesterol depletion and increased by cold. One might predict that opposite effects on cell rigidity should have opposite effects on the probability of wounding (8, 24, 29); however, our findings show that both interventions resulted in an increase in cell wounding. Cholesterol depletion, low temperature, and cytoskeletal alteration all had one effect in common: inhibition of DILT. Thus, together, these results suggest that the mechanical properties of the cell's stress-bearing elements (namely the plasma membrane and the cytoskeleton) are less of a determinant of plasma membrane wounding than is DILT, a process that actively remodels the stress-bearing capability of the cell. Of note, cellular tensegrity does not account for such active remodeling of cellular stress-bearing elements (30). These results also point out that the cytoskeleton is not solely a structural force-bearing unit of the cell but rather is integrally involved in facilitating signal transduction and vesicle trafficking between organelles and the plasma membrane (31–33). Also, it would seem that the rate at which the cell is able to remodel its stress-bearing elements will determine the probability of wounding. This supposition is indeed supported by our findings that wounding is increased with increasing strain rate.

Not only was wounding found to be increased with inhibition of DILT, but concomitantly, the rate of wound resealing was found to be decreased. The mechanisms of cell wound repair have been studied extensively and reviewed recently (11, 12, 21). It has been postulated that resealing can occur either spontaneously by passive lateral diffusion of lipid molecules within the injured plasma membrane edges or by "patch" resealing via rapid fusion of lipid vesicles into a large "lipid patch" in close proximity to the wound (12) or exocytosis of intracellular lipid resulting in decreased plasma membrane tension (8, 25). Our results show that wound resealing in alveolar epithelial cells

involves a vesicular process of exocytosis that is independent of the mechanical properties of either the plasma membrane or the cytoskeleton. They also highlight the conflicting literature regarding the importance of an intact actin cytoskeleton for facilitation of wound resealing (34).

The motivation for these studies is the clinical entity of ventilator-induced lung injury. Numerous studies have focused on the manifestations and physiologic consequences of ventilator-induced lung injury in animal models and humans. The cytopathologic lesions of ventilator-induced lung injury, namely plasma membrane blebbing, intercellular and intracellular epithelial and endothelial gap formation, and denudation of the basement membrane have all been carefully documented, yet research on the pathophysiology and molecular mechanisms of mechanical lung injury has focused largely on downstream events such as edema formation and inflammation, which are consequences of cellular mechanotransduction and stress failure. Comparatively little is known about the actual deformation experienced by lung cells during mechanical ventilation, nor have the adaptive responses of lung cells to deforming stresses been rigorously defined.

In this study, we chose to elucidate alveolar epithelial cell injury and repair mechanisms in an *in vitro* setting. Although repeated deformation has obvious direct relevance to mechanical ventilation, we chose a single, held stretch because it was simple and addressed basic and broad unanswered questions about alveolar epithelial cell mechanics and deformation-related remodeling. The cytoskeleton is the principal stress-bearing element of the plasma membrane, a source of mechanosensing, an avenue for transport of proteins and lipid cargo, and actively remodels in response to deformation; however, the quasi-static mechanical properties of the cytoskeleton did not predict the susceptibility of cells to deformation injury. Rather, our observations are consistent with the hypothesis that a deformed cell unable to actively regulate its surrounding lipid bilayer cannot keep bilayer tension below lytic levels. This remodeling and cell plasticity, as opposed to the inherent static mechanical properties of the cytoskeleton, determine the fate of a cell that is forced to assume a certain shape. The concept is akin to the volutrauma idea. Dreyfuss and Saumon (4) and Hernandez and colleagues (35) showed that pressure applied to the airway is damaging to the lung only if this pressure causes a large lung volume excursion. Scaled down to the individual cell, this means that for a given external force, a "rigid" cytoskeleton simply prevents a large shape change from occurring; however, when the deformation of the surrounding matrix, for example, the basement membrane, imposes a large cell strain then having a rigid cytoskeleton simply means that a large deforming stress will be generated. Such a stress could become lytic to a "weak" structure, causing it to fail. Remodeling of stress bearing elements (the cytoskeleton) or of potentially stress bearing elements (the lipid bilayer of the plasma membrane) is the principal mechanism by which the cell can protect itself from such a catastrophic event.

Because remodeling is a rate-dependent process, one might speculate that the dependence of wounding on strain rate reflects limits in the rate at which lipid vesicles can be transported to and fuse with the plasma membrane. It could also reflect limits in the rate at which the subcortical cytoskeleton can remodel. More work will need to be done to define the relevant rate constants. The observation that strain rate, not just strain amplitude, is an important determinant of cell injury might also have clinical relevance on the appropriate choice of flow and rate settings during mechanical ventilation. The most important message of our work, however, is that mechanisms of deformation-related cell remodeling such as DILT are appropriate and under-

appreciated treatment targets in the search for pharmacoprotective agents against ventilator-induced lung injury.

Acknowledgment: The authors thank Dr Gary C. Sieck for use and help with confocal microscopy and Dr. Vishwajeet Puri for help with cholesterol quantification.

References

1. Stroetz RW, Vlahakis NE, Walters BJ, Schroeder MA, Hubmayr RD. Validation of a new live cell strain system: characterization of plasma membrane stress failure. *J Appl Physiol* 2001;90:2361–2370.
2. Tschumperlin DJ, Margulies SS. Equibiaxial deformation-induced injury of alveolar epithelial cells in vitro. *Am J Physiol* 1998;275:L1173–L1183.
3. Vlahakis NE, Hubmayr RD. Cellular responses to mechanical stress. invited review: plasma membrane stress failure in alveolar epithelial cells. *J Appl Physiol* 2000;89:2490–2496.
4. Dreyfuss D, Saumon G. Ventilator-induced lung injury: lessons from experimental studies. *Am J Respir Crit Care Med* 1998;157:294–323.
5. Fu Z, Costello ML, Tsukimoto K, Prediletto R, Elliott AR, Mathieu-Costello O, West JB. High lung volume increases stress failure in pulmonary capillaries. *J Appl Physiol* 1992;73:123–133.
6. Tschumperlin DJ, Margulies SS. Alveolar epithelial surface area-volume relationship in isolated rat lungs. *J Appl Physiol* 1999;86:2026–2033.
7. Vlahakis NE, Schroeder MA, Pagano RE, Hubmayr RD. Deformation-induced lipid trafficking in alveolar epithelial cells. *Am J Physiol Lung Cell Mol Physiol* 2001;280:L938–L946.
8. Dai J, Sheetz MP, Wan X, Morris CE. Membrane tension in swelling and shrinking molluscan neurons. *J Neurosci* 1998;18:6681–6692.
9. Raucher D, Sheetz MP. Characteristics of a membrane reservoir buffering membrane tension. *Biophys J* 1999;77:1992–2002.
10. Lin Y-C, Ho C-H, Grinnell F. Fibroblasts contracting collagen matrices form transient plasma membrane passages through which the cells take up fluorescein isothiocyanate-dextran and Ca^{2+} . *Mol Biol Cell* 1997;8:59–71.
11. McNeil PL, Steinhart RA. Loss, restoration and maintenance of plasma membrane integrity. *J Cell Biol* 1997;137:1–4.
12. McNeil PL, Terasaki M. Coping with the inevitable: how cells repair a torn surface membrane. *Nat Cell Biol* 2001;3:E124–E129.
13. Bi G-Q, Morris RL, Liao G, Alderton JM, Scholey JM, Steinhart RA. Kinesin- and myosin-driven steps of vesicle recruitment for Ca^{2+} -regulated exocytosis. *J Cell Biol* 1997;138:999–1008.
14. Terasaki M, Miyake K, McNeil PL. Large plasma membrane disruptions are rapidly resealed by Ca^{2+} -dependent vesicle-vesicle fusion events. *J Cell Biol* 1997;139:63–74.
15. Hanson DP, Robb RA, Aharon S, Augustine KE, Cameron BM, Camp JJ, Karwoski RA, Larson AG, Stacy MC, Workman EL. New software toolkits for comprehensive visualization and analysis of three-dimensional multimodal biomedical images. *J Digit Imaging* 1997;10:229–230.
16. Berrios JC, Schroeder MA, Hubmayr RD. Mechanical properties of alveolar epithelial cells in culture. *J Appl Physiol* 2001;91:65–73.
17. Wang N, Butler JP, Ingber DE. Mechanotransduction across the cell surface and through the cytoskeleton. *Science* 1993;260:1124–1127.
18. Reddy A, Caler EV, Andrews NW. Plasma membrane repair is mediated by Ca^{2+} -regulated exocytosis of lysosomes. *Cell* 2001;106:157–169.
19. Grembowicz KP, Sprague D, McNeil PL. Temporary disruption of the plasma membrane is required for c-fos expression in response to mechanical stress. *Mol Biol Cell* 1999;10:1247–1257.
20. Paine R III, Simon RH. Expanding the frontiers of lung biology through the creative use of alveolar epithelial cells in culture. *Am J Physiol* 1996;14:L484–L486.
21. Hamill OP, Martinac B. Molecular basis of mechanotransduction in living cells. *Physiol Rev* 2001;81:685–740.
22. Wirtz HR, Dobbs LG. The effects of mechanical forces on lung functions. *Respir Physiol* 2000;119:1–7.
23. Chicurel ME, Singer RH, Meyer CJ, Ingber DE. Integrin binding and mechanical tension induce movement of mRNA and ribosomes to focal adhesions. *Nature* 1998;392:730–733.
24. Morris CE, Homann U. Cell surface area regulation and membrane tension. *J Membr Biol* 2001;179:79–102.
25. Sheetz MP, Dai J. Modulation of membrane dynamics and cell motility by membrane tension. *Trends Cell Biol* 1996;6:85–89.
26. Glogauer M, Arora P, Chou D, Janmey PA, Downey GP, McCulloch CAG. The role of actin-binding protein 280 in integrin-dependent mechanoprotection. *J Biol Chem* 1998;273:1689–1698.
27. Geiger B, Bershadsky A, Pankov R, Yamada KM. Transmembrane crosstalk between the extracellular matrix–cytoskeleton crosstalk. *Nat Rev Mol Cell Biol* 2001;2:793–805.
28. Lewis SA, de Moura JL. Incorporation of cytoplasmic vesicles into apical membrane of mammalian urinary bladder epithelium. *Nature* 1982;297:685–688.
29. Herring TL, Slotin IM, Baltz JM, Morris CE. Neuronal swelling and surface area regulation: elevated intracellular calcium is not a requirement. *Am J Physiol* 1998;274:C272–C281.
30. Ingber DE. Tensegrity: the architectural basis of cellular mechanotransduction. *Annu Rev Physiol* 1997;59:575–599.
31. Janmey PA. The cytoskeleton and cell signaling: component localization and mechanical coupling. *Physiol Rev* 1998;78:763–781.
32. Suter DM, Forscher P. Transmission of growth cone traction force through apCAM-cytoskeletal linkages is regulated by Src family tyrosine kinase activity. *J Cell Biol* 2001;155:427–438.
33. Yeaman C, Grindstaff KK, Wright JR, Nelson WJ. Sec6/8 complexes on trans-Golgi network and plasma membrane regulate stages of exocytosis in mammalian cells. *J Cell Biol* 2001;155:593–604.
34. Miyake K, McNeil PL, Suzuki K, Tsunoda R, Sugai N. An actin barrier to resealing. *J Cell Sci* 2001;114:3487–3494.
35. Hernandez LA, Peevy KJ, Moise AA, Parker JC. Chest wall restriction limits high airway pressure-induced lung injury in young rabbits. *J Appl Physiol* 1989;66:2364–2368.